10-12-2007

Characterization of MazFSa, an Endoribonuclease from Staphylococcus aureus

Zhibiao Fu
Dartmouth College

Niles P. Donegan
Dartmouth College

Guido Memmi
Dartmouth College

Ambrose L. Cheung
Dartmouth College

JOURNAL OF BACTERIOLOGY, Dec. 2007, p. 8871–8879 Vol. 189, No. 24
0021-9193/07/$08.00+0 doi:10.1128/JB.01272-07

Characterization of $MazF_{Sa}$, an Endoribonuclease from *Staphylococcus aureus*▽

Zhibiao Fu, Niles P. Donegan, Guido Memmi, and Ambrose L. Cheung*

Department of Microbiology and Immunology, Dartmouth Medical School, Hanover, New Hampshire 03755

Received 7 August 2007/Accepted 2 October 2007

The *mazEF* homologs of *Staphylococcus aureus*, designated $mazEF_{sa}$, have been shown to cotranscribe with the *sigB* operon under stress conditions. In this study, we showed that $MazEF_{Sa}$, as with their *Escherichia coli* counterparts, compose a toxin-antitoxin module wherein $MazF_{Sa}$ leads to rapid cell growth arrest and loss in viable CFU upon overexpression. $MazF_{Sa}$ is a novel sequence-specific endoribonuclease which cleaves mRNA to inhibit protein synthesis. Using *ctpA* mRNA as the model substrate both in vitro and in vivo, we demonstrated that $MazF_{Sa}$ cleaves single-strand RNA preferentially at the 5′ side of the first U or 3′ side of the second U residue within the consensus sequences VUUV′ (where V and V′ are A, C, or G and may or may not be identical). Binding studies confirmed that the antitoxin $MazE_{Sa}$ binds $MazF_{Sa}$ to form a complex to inhibit the endoribonuclease activity of $MazF_{Sa}$. Contrary to the system in *E. coli*, exposure to selected antibiotics augmented $mazEF_{sa}$ transcription, akin to what one would anticipate from the environmental stress response of the *sigB* system. These data indicate that the *mazEF* system of *S. aureus* differs from the gram-negative counterparts with respect to mRNA cleavage specificity and antibiotic stresses.

Many bacteria have chromosomally encoded toxin-antitoxin (TA) loci, in which the toxin and antitoxin genes exist in an operon and are coexpressed together to form a TA complex. The toxin is stable, whereas the antitoxin is a labile protein degraded in vivo by host proteases (e.g., Clp or Lon in *Escherichia coli*). Under conditions that preclude the continuous synthesis of the antitoxin, the toxin can exert its toxic effect to inhibit cell growth (7, 9, 12). There are at least eight typical TA families known in prokaryotes (12, 21). Among these, the MazEF and RelBE systems from *E. coli* have been the most extensively studied (7, 9, 12). Structural studies have disclosed that the MazE-MazF complex in *E. coli* consists of two MazF dimers and one MazE dimer in a hexameric $MazF_2$-$MazE_2$-$MazF_2$ configuration (17). In contrast, the RelBE complex from *Pyrococcus horikochi* is a $(RelE\text{-}RelB)_2$ tetramer (32).

Inhibition of protein synthesis by MazF in *E. coli* has been found to be attributable to cleavage of cellular mRNA. More specifically, MazF in *E. coli* is a sequence-specific endoribonuclease, cleaving mRNA at ACA sites independently of ribosomes both in vitro and in vivo (6, 34). The cleavage occurs at the 5′ end of ACA sequence to yield a 2′,3′-cyclic phosphate as part of the end product. The 2′-OH group of the nucleotide preceding the ACA sequence is essential for MazF cleavage (37). In contrast, the RelE toxin of *E. coli* was found to cleave mRNA positioned at the ribosomal A-site both in vitro and in vivo (26). Cleavage occurs between the second and third bases of the A-site codon (UAH, where H is usually G or A), with the cleavage efficiency depending on the specific codon at the ribosomal A-site. For instance, UAG and UAA are cleaved more efficiently than the UGA stop codon (26). The toxin systems from other prokaryotes also appeared to represent sequence-specific endoribonucleases. The PemK toxin from plasmid R100 in *E. coli* cleaves mRNA at UAH (where H is A, C, or U) (36), and ChpBK cleaves at ACY (where Y is A, G, or U) in a single-stranded RNA (38), while the *Bacillus subtilis* MazF homolog EndoA cleaves mRNA at a UAC sequence (27). Recently, two MazF homologs from *Mycobacterium tuberculosis* were also found to be endoribonucleases. One of the MazF homologs from *M. tuberculosis* cleaves mRNA at UAC triplets, while the other homolog cleaves U-rich regions within mRNA (39).

In examining the *sigB* operon of *Staphylococcus aureus*, Kullik et al. (18) noted that an open reading frame (ORF) immediately upstream of the *sigB* operon may encode a *mazF* homolog (designated the *pemK* homolog). Senn et al. (30) subsequently demonstrated that the *sigB* operon in *S. aureus* strain COL comprises two additional ORFs (SA2059 and SA2058) in addition to *rsbU*, *rsbV*, *rsbW*, and *sigB*. They also observed, as did Gertz et al. (13), that SA2058 and, to a much lesser extent, SA2059 share some degree of homology with MazF and MazE of *E. coli*, respectively. SA2059 and SA2058 are cotranscribed with the *sigB* operon under stress conditions, such as heat and high-salt conditions (30). For brevity and consistency, we propose to name SA2059 and SA2058 (designated as SA1873 and SAS067 in N315) in COL as $MazE_{Sa}$ and $MazF_{Sa}$, respectively, in *S. aureus*. Although it has been hinted that the *S. aureus* $MazEF_{Sa}$ may act as a TA module (30), there have been no experimental data supporting this hypothesis. This confusion has been generated in part as a consequence of a general lack of protein sequence similarity between $MazE_{Sa}$ and its *E. coli* counterpart.

In this study, we provide definitive evidence that $MazEF_{Sa}$ is a TA module in *S. aureus*, with $MazF_{Sa}$ as the toxin. Our data demonstrate that $MazF_{Sa}$ is a sequence-specific endoribonuclease which cleaves *ctpA* mRNA at a consensus U-rich sequence of VUUV′ (where V and V′ are A, C, or G and may

* Corresponding author. Mailing address: Department of Microbiology and Immunology, Dartmouth Medical School, Hanover, NH 03755. Phone: (603) 676-3350, ext. 2. Fax: (603) 676-3355. E-mail: Ambrose.Cheung@Dartmouth.edu.

▽ Published ahead of print on 12 October 2007.

or may not be identical) both in vivo and in vitro. $MazF_{Sa}$ showed high cellular toxicity in both *E. coli* and *S. aureus* upon induction and inhibited protein synthesis in a cell-free system. Collectively, our results suggest that the activated $MazEF_{Sa}$ TA module cleaves mRNA cleavage at a specific site under stressful conditions to affect translation. This finding raises the possibility that inhibition of $MazE_{Sa}$ may represent a novel approach to antibacterial therapy for *S. aureus*.

MATERIALS AND METHODS

Bacterial strains and culture conditions. We used *E. coli* strains DH5α and BL21(DE3)pLysS and *S. aureus* strains Newman and 178RI (8) for these studies. *S. aureus* 178RI carries an isopropyl-β-D-thiogalactopyranoside (IPTG)-inducible T7 polymerase gene integrated into the *geh* locus in the chromosome of RN4220. For transduction, phage ϕ85 was used to produce phage lysates of *S. aureus* 178RI. The phage lysate was then used to infect *S. aureus* Newman as described elsewhere (3) to obtain the *S. aureus* transductant ACL6094 carrying the T7 polymerase gene integrated into the chromosome in the Newman background. Cultures were routinely grown in LB for *E. coli* and in 03GL or trypticase soy broth for *S. aureus* with aeration at 37°C. The media were supplemented with either ampicillin (Amp; 70 μg/ml) or chloramphenicol (Cm; 10 μg/ml).

Construction of plasmids. The $mazE_{Sa}$ (GenBank accession number Y16431) and $mazF_{Sa}$ (GenBank accession number Y07645) genes were amplified by PCR using *S. aureus* Newman genomic DNA as a template and cloned into the NcoI and BamHI sites of cloning vectors pCDF1 and pET14b (Novagen) in *E. coli* to make pCDF1-MazE$(His)_6$ and pET14b-MazF$(His)_6$ with the His_6 tag at the N terminus, respectively. The $mazE_{sa}$ gene without the His tag was amplified by PCR and cloned into the NdeI/XhoI sites of pETDuet1 (Novagen). An NcoI-BamHI-digested DNA fragment from pET14b-MazF$(His)_6$ was then inserted to make pETDuet1-MazEF$(His)_6$ with the His_6 tag only at the $MazF_{Sa}$ N terminus. An NcoI-BamHI- and a BglII-EcoRI-digested DNA fragment from pET14b-MazF$(His)_6$ was further cloned into NcoI- and BamHI-digested pBAD22 (14) and BglII-EcoRI-digested pG164 (8), respectively, to generate pBAD22-MazF$(His)_6$ and pG164-MazF$(His)_6$. The *ctpA* gene (encoding a carboxy-terminal protease from *S. aureus*; GenBank accession number NP_374534) was also amplified by PCR using *S. aureus* Newman genomic DNA as the template and cloned into the NcoI and BamHI sites of pET14b (Novagen) to produce pET14b-ctpA. A BglII-EcoRI-digested fragment from pET14b-ctpA was further cloned into BamHI- and EcoRI-digested pG164-MazF$(His)_6$ to generate pG164-MazF$(His)_6$/ctpA. DNA techniques were performed according to standard procedures (28).

Protein expression and purification. MazE$(His)_{6Sa}$ was expressed in *E. coli* BL21(DE3)pLysS carrying the plasmid pCDF1-MazE$(His)_6$ under IPTG induction (1 mM) for 4 h. For MazF$(His)_{6Sa}$ expression, the $MazE_{Sa}$ and MazF$(His)_{6Sa}$ genes were coexpressed in *E. coli* BL21(DE3)pLysS harboring the plasmid pETDuet1-MazEF$(His)_6$ after IPTG induction (1 mM) for 6 h. The cells were harvested and subjected to lysis by ultrasonication. MazE$(His)_{6Sa}$ and MazE-MazF$(His)_{6Sa}$ complex were purified with a nickel-nitrilotriacetic acid resin affinity column (Novagen) according to the manufacturer's protocol. MazF$(His)_{6Sa}$ was further purified from the MazE-MazF$(His)_{6Sa}$ complex as described previously (35). In brief, $MazE_{Sa}$ was dissociated from MazF$(His)_{6Sa}$ in the purified MazE-MazF$(His)_{6Sa}$ complex with 6 M guanidine HCl. MazF$(His)_{6Sa}$ was retrapped with the nickel-nitrilotriacetic acid resin affinity column, eluted, and refolded by stepwise dialysis as described previously (25).

Native PAGE. Various amounts of MazE$(His)_{6Sa}$ and MazF$(His)_{6Sa}$ were mixed in binding buffer (50 mM Tris-HCl, pH 7.5, 5 mM $MgCl_2$, 1 mM dithiothreitol, and 5% glycerol) at 4°C for 30 min and subjected to native polyacrylamide gel electrophoresis (PAGE) analysis in running buffer containing 82.6 mM Tris-HCl (pH 9.4) and 33 mM glycine as described previously (35). The protein bands were visualized by staining with Coomassie brilliant blue.

Primer extension analyses. For in vitro primer extension, the *ctpA* mRNA was transcribed from BamHI-linearized pET14b-ctpA plasmid, using the T7 large-scale transcription kit (Promega) according to the manufacturer's protocol. Five μg of *ctpA* mRNA was partially digested with 15 pmol of $MazF_{Sa}$ in a 20-μl reaction mixture containing 40 U of RNase inhibitor, 50 mM Tris-HCl (pH 8.0), 50 mM NaCl, and 1 mM dithiothreitol at 37°C for 90 min. The digestion mixture was then extracted with phenol-chloroform followed by ethanol precipitation to remove the proteins. Primer extension (Promega primer extension kit) analysis of the digested mRNA was carried out with labeled primers pEa d(GCTTGAT CAGTTTTGTTTAAACCAC), pEb d(TGACCATGCCATCAATTGCAGC), pEc d(AGGACGAATGCCAGCACGTTCTGCTGG), and pEd d(CTTCACT ACCT CGTTGAACAGTTA), following the manufacturer's protocol. The primers were 5′-end labeled with [γ-^{32}P]ATP using T4 polynucleotide kinase. For in vivo primer extension analysis of *ctpA* mRNA cleavage sites in *E. coli*, we isolated total cellular RNA from *E. coli* BL21(DE3)pLysS cells harboring both pBAD22-MazF$(His)_6$ and pET14b-ctpA. Cultures were induced with 1 mM IPTG to transcribe the *ctpA* mRNA for 30 min. $MazF_{Sa}$ was then induced by adding arabinose to a final concentration of 0.2%. For in vivo primer extension in *S. aureus*, 178RI harboring pG164-MazF$(His)_6$/ctpA was induced with 1 mM IPTG. The *ctpA* mRNA was cotranscribed with the $mazF_{Sa}$ mRNA. After induction, total cellular RNA from a 10-ml culture was then extracted at the indicated time point as described previously (4). Trace DNA was further removed by digestion with RNase-free DNase I (Roche) followed by extraction with phenol-chloroform and ethanol precipitation to clean the RNA. Primer extension was then carried out with different primers as described previously (16). The primer extension product was analyzed on a 6% sequencing gel with the DNA sequencing ladder prepared with the same primer running side by side, followed by autoradiography.

Cleavage of synthetic RNAs by $MazF_{Sa}$. All RNAs were commercially synthesized (IDT, Coralville, IA) and 5′-end labeled with [γ-^{32}P]ATP using T4 polynucleotide kinase. The native sequence, 5′-UUGGCAAUUCAUAUCAAU-3′, corresponding to the sense RNA, was named AUUC, with AUUC as the target cleavage site. Seven other RNA substrates with the center AUUC sequences changed to AGUC, AUGC, AUUU, UUUC, AUUG, GUUC, and GUUG sequences were also synthesized and named AGUC, AUGC, AUUU, UUUC, AUUG, GUUC, and GUUG, respectively. The synthesized native DNA sequence, 5′-TTGGCAATTCATATCAAT-3′, named ATTC, was used as a control. A 19-base synthetic RNA (5′-UGCAAUUCAUAUGAAUUGU-3′) that can form hairpin structure with the AUUC sequence located in the duplex region was named RB-1. Another 19-base RNA (5′-UGCAAUUCAUAUCAAUAU G-3′), which cannot form the hairpin structure, was named RB-2. An antisense RNA to the native AUUC RNA sequence (5′-AUUGAUAUGAAUUGCCA A-3′), was named RB-3. The labeled RNA substrates were digested with $MazF_{Sa}$ at 37°C for 30 min in a 10-μl reaction mixture containing 20 U of RNase inhibitor, 15 pmol of $MazF_{Sa}$, 1 pmol labeled RNA, and 10 mM Tris-HCl (pH 7.9). The formation of RNA-RNA duplex with the sense RNA AUUC and RB-3-, the antisense RNA-, or $MazF_{Sa}$-mediated cleavage was analyzed as described elsewhere (36). Briefly, 1 pmol of labeled sense RNA was annealed with its antisense RNA in different ratio combinations and incubated with 15 pmol of $MazF_{Sa}$ at 37°C for 30 min. The reactions were stopped by adding loading buffer and analyzed by separating on a 20% sequencing gel. The RNA ladder was prepared by partial alkaline hydrolysis (Ambion) of the 5′-end-labeled 18-base sense RNA, AUUC, according to the manufacturer's protocol.

Northern blot hybridization. Total RNA from *S. aureus* was prepared by using a TRIzol isolation kit (Invitrogen, CA) and a reciprocating shaker (4). For detection of specific transcripts, gel-purified DNA probes were radiolabeled with [α-^{32}P]dCTP by use of a random-primed DNA labeling kit (Roche Diagnostics GmbH) and hybridized under aqueous-phase conditions at 65°C. The blots were subsequently washed with 2× SSC (1× SSC is 0.15 M NaCl plus 0.015 M sodium citrate), 0.1% sodium dodecyl sulfate (SDS) twice at room temperature and 1× SSC, 0.1% SDS twice at 65°C and autoradiographed as previously described (20).

Bacterial viability assay. Bacteria were stained with the membrane-permeable SYTO9 and the membrane-impermeable propidium iodide using the Live/Dead *Bac*Light bacterial viability kit (Molecular Probes, Eugene, OR) and quantitated with fluorescence microplate readers according to the manufacturer's protocol. Bacteria with intact cell membranes stain fluorescent green, whereas bacteria with damaged membranes stain fluorescent red.

RESULTS

$MazEF_{Sa}$ is a TA module in *S. aureus*. A BLAST search of SA2058, encoding a 120-residue protein in the COL genome, identified this gene to have 20% identity and 40% similarity to the *E. coli* MazF protein. The upstream gene SA2059, which is cotranscribed with SA2058, encodes a 56-residue protein with only 12% identity and 21% similarity to the *E. coli* MazE protein. We have named SA2058 and SA2059 $MazF_{Sa}$ and $MazE_{Sa}$ for brevity and clarity, which were referred to by Mittenhuber (21) as Orf136-s.a and Orf6-s.a (Fig. 1A).

To examine if $MazF_{Sa}$ and $MazE_{Sa}$ function as a TA module,

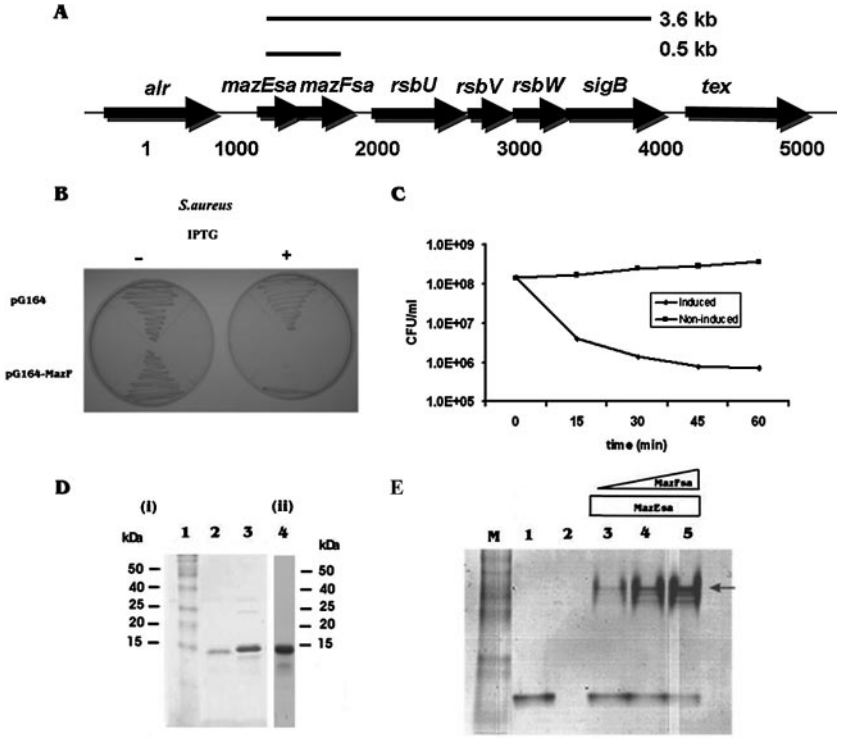

FIG. 1. Inhibition of cell growth by *S. aureus* MazF$_{Sa}$. (A) Schematic representation of genetic organization of the *S. aureus mazEF$_{Sa}$* and *sigB* operons. (B) *S. aureus* ACL6094 cells were transformed with pG164-MazF(His)$_6$. The cells were then streaked on a 03GL agar plate with or without induction with IPTG (1 mM) followed by incubation overnight at 37°C. (C) Reduction of CFU with *S. aureus* ACL6094 harboring pG164-MazF(His)$_6$ under induction. The cultures were induced at an optical density at 650 nm of 0.4 with IPTG (1 mM). To determine the CFU, samples were withdrawn at various time points, spread on TSA plates supplemented with chloramphenicol (10 μg/ml), and incubated at 37°C overnight. (D) Characterization of MazE$_{Sa}$/MazF$_{Sa}$. The MazE(His)$_{6Sa}$ and MazF(His)$_{6Sa}$ proteins were purified as described in Materials and Methods. The proteins were analyzed by 16% SDS-PAGE. (i) lane 1, protein molecular mass markers; lane 2, MazE(His)$_{6Sa}$; lane 3, MazF(His)$_{6Sa}$; (ii) lane 4, purified MazE-MazF(His)$_{6Sa}$ complex. The upper band is MazF(His)$_{6Sa}$, and the lower band is the copurified MazE$_{Sa}$. (E) Native PAGE analysis of MazEF$_{Sa}$ complex formation. MazE(His)$_{6Sa}$ was mixed with MazF(His)$_{6Sa}$ as described in Materials and Methods and subjected to native PAGE analysis. Lane M, molecular mass markers; lane 1, MazE(His)$_{6Sa}$ (32 pmol); lane 2, MazF(His)$_{6Sa}$ (30 pmol); lanes 3 to 5, MazE(His)$_{6Sa}$ (32 pmol). Samples were mixed with 7.5 pmol, 15 pmol, and 30 pmol of MazF(His)$_{6Sa}$, respectively. The MazE$_{Sa}$/MazF$_{Sa}$ complex is indicated by the arrow.

we determined whether the MazF$_{Sa}$ protein, when expressed independently, is toxic to bacterial cells. For this purpose, the *mazF$_{Sa}$* gene was cloned into the vector pBAD with an arabinose-inducible promoter and the shuttle vector pG164 with an IPTG-inducible promoter to generate pBAD-MazF(His)$_6$ and pG164-MazF(His)$_6$, respectively, as described in Materials and Methods. The growth of *S. aureus* ACL6094 carrying the plasmid pG164-MazF(His)$_6$ with a T7-dependent promoter was inhibited on 03GL agar plates supplemented with IPTG (1 mM) but not in the unsupplemented control (Fig. 1B). Time course studies were further carried out to characterize the toxicity of MazF$_{Sa}$. We found that most of the cells with the *mazF$_{Sa}$* operon cloned into pG164 could not yield colonies on nutrient agar plates after induction for 60 min, while cells without induction showed normal growth (Fig. 1C). Although the CFU counts were reduced 99.5% after 60 min postinduction, fewer than 5% of the cells stained positively with propidium iodide (Molecular Probes, Eugene, OR), a dye which binds membrane-compromised dead bacteria (data not shown), thus indicating MazF$_{Sa}$ expression mainly induced bacterial stasis and hence a defect in replication. Similar results occurred in *E. coli* with the plasmid pBAD-MazF(His)$_6$ (data not shown). In contrast, *E. coli* and *S. aureus* cells with *mazEF$_{Sa}$* cloned into pBAD and pG164, respectively, exhibited normal growth even under respective induction (arabinose or IPTG) (data not shown). Together, these data demonstrated that MazF$_{Sa}$ is toxic to both *E. coli* and *S. aureus* and that this toxicity can be reversed by coexpression of MazE$_{Sa}$ with MazF$_{Sa}$.

To further characterize the MazEF$_{Sa}$ TA module, we expressed and purified MazF(His)$_{6Sa}$ and MazE(His)$_{6Sa}$ (both N-terminally tagged) (Fig. 1D) in *E. coli* as described in Materials and Methods. MazE(His)$_{6Sa}$ and MazF(His)$_{6Sa}$ were mixed together in a dose-dependent manner and subjected to native PAGE analysis. Despite the noticed migration of MazE(His)$_{6Sa}$ (pI 4.2), no obvious mobility was observed for MazF(His)$_{6Sa}$ alone (Fig. 1E, lane 2), presumably due to its basic pI (9.5), which approaches the pH (9.4) of the running buffer used in native PAGE. Nevertheless, the MazEF$_{Sa}$ complex, appearing as a higher-molecular-weight species than that of MazE(His)$_{6Sa}$ alone, was observed at the top of the gel (Fig. 1E, lanes 3 to 5). The quantity of the MazEF$_{Sa}$ complex rose with increasing concentrations of MazF(His)$_{6Sa}$, while the amount of free MazE(His)$_{6Sa}$ at the bottom of the gel continued to diminish (Fig. 1E). These results indicated that MazE$_{Sa}$ and MazF$_{Sa}$, as a paired TA module, interact in vitro and possibly in vivo.

MazF$_{Sa}$ inhibits protein synthesis in a cell-free system. We then examined the effect of the purified MazF$_{Sa}$ on protein syn-

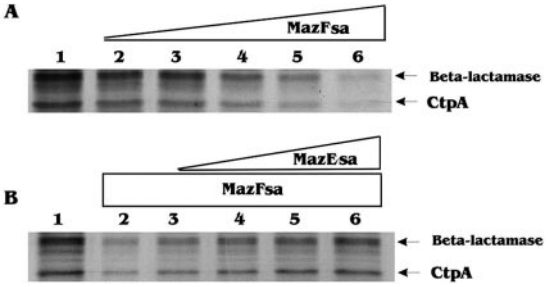

FIG. 2. Effects of $MazF_{Sa}$ and $MazE_{Sa}$ on cell-free protein synthesis. (A) Inhibition of protein synthesis by $MazF_{Sa}$. Protein synthesis was carried out with the plasmid pET14b-ctpA in an *E. coli* T7 S30 extract system at 37°C for 1 h. Lane 1, control without $MazF_{Sa}$; lanes 2 to 6, various amounts of $MazF_{Sa}$ were added at 3.75 pmol, 7.5 pmol, 11.25 pmol, 15 pmol, and 30 pmol, respectively. (B) Protein synthesis was rescued by the addition of $MazE_{Sa}$. Lane 1, control without $MazF_{Sa}$; lane 2, 15 pmol of $MazF_{Sa}$; lanes 3 to 6, 8 pmol, 16 pmol, 32 pmol, or 64 pmol of $MazE_{Sa}$, respectively, was added together with 15 pmol of $MazF_{Sa}$. The synthesis of β-lactamase and CtpA are indicated by arrows.

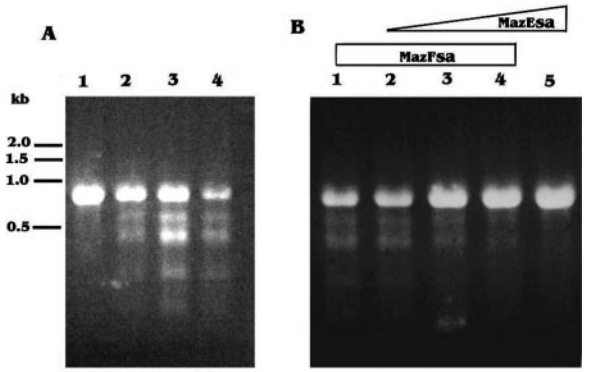

FIG. 3. Endoribonuclease activity of $MazF_{Sa}$. Five μg of *ctpA* mRNA was digested with 15 pmol of $MazF_{Sa}$ as described in Materials and Methods. (A) Cleavage of *ctpA* mRNA by $MazF_{Sa}$. Lane 1, control without $MazF_{Sa}$; lanes 2 to 4, mRNA substrates were digested for 60 min, 90 min, and 120 min, respectively. (B) Inhibition of cleavage with the addition of $MazE_{Sa}$. Lane 1, mRNA with $MazF_{Sa}$; lanes 2 to 4, mRNA substrates digested by $MazF_{Sa}$ together with 4 pmol, 8 pmol, or 16 pmol of $MazE_{Sa}$; lane 5, mRNA with 32 pmol of $MazE_{Sa}$.

thesis in a cell-free system. The synthesis of the truncated CtpA protein (~15 kDa), representing part of the carboxy-terminal protease from *S. aureus*, from the plasmid pET14b-ctpA was carried out at 37°C for 1 h using an *E. coli* T7 S30 extract system with and without $MazF_{Sa}$ (Fig. 2A). The synthesis of CtpA was inhibited with increasing concentrations of $MazF_{Sa}$ and was almost completely blocked with 30 pmol added (Fig. 2A). Addition of $MazE_{Sa}$ to the cell-free system containing $MazF_{Sa}$ rescued CtpA synthesis in a dose-dependent manner (Fig. 2B). As expected, the $MazF_{Sa}$ protein also inhibited the synthesis of β-lactamase from the *bla* gene present in the pET14b-ctpA vector in *E. coli* (Fig. 2). Preincubation of the *E. coli* cell-free protein synthesis system with $MazF_{Sa}$ for 20 min at 37°C prior to adding the plasmid pET14b-ctpA and $MazE_{Sa}$ did not have any significant effect on subsequent CtpA synthesis (data not shown). These results suggest that the primary target for $MazF_{Sa}$ is not the ribosome, tRNA, or other factors required for protein synthesis in this system, but rather the mRNA of the cell.

In vitro cleavage of *ctpA* mRNA by $MazF_{Sa}$. To determine whether $MazF_{Sa}$ has endoribonuclease activity, we prepared the *ctpA* mRNA using an in vitro transcription system as described in Materials and Methods. The *ctpA* mRNA was then incubated with $MazF_{Sa}$ in a dose- and time-dependent manner. As shown in Fig. 3A, the *ctpA* mRNA was cleaved into small fragments with 15 pmol of $MazF_{Sa}$ in a time-dependent manner, while the addition of $MazE_{Sa}$ inhibited the digestion of *ctpA* mRNA by $MazF_{Sa}$ in a dose-dependent fashion (Fig. 3B). These results demonstrate that $MazF_{Sa}$ is an endoribonuclease that cleaves mRNA to inhibit protein synthesis and that $MazE_{Sa}$ functions as an antitoxin to counteract the endoribonuclease activity of $MazF_{Sa}$.

The *ctpA* mRNA was noted to be cleaved into distinct, but not smearing, bands by $MazF_{Sa}$ (Fig. 3A), indicating that $MazF_{Sa}$ may be a sequence-specific endoribonuclease. To further map the cleavage site, we employed $MazF_{Sa}$ to partially digest the *ctpA* mRNA and then subjected the digest to primer extension, using four different DNA primers, pEa to -d, covering the experimental *ctpA* mRNA as described in Materials and Methods. To determine the cleavage sites, each primer extension product was analyzed on a 6% sequencing gel with a DNA sequencing ladder prepared with the same primer (Fig. 4). The cleavage sites in the *ctpA* mRNA as determined by primer extension studies are shown in Table 1. Cleavages occurred preferentially in a U-rich region with a consensus sequence of VUUV′ in *ctpA* mRNA. The UU dinucleotides were found to be conserved among all cleavage sites. However, the

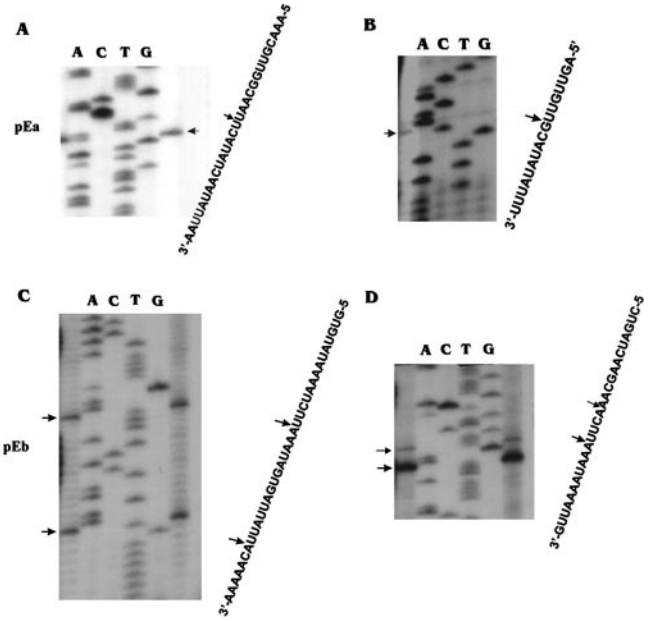

FIG. 4. In vitro primer extension analysis of the $MazF_{Sa}$ cleavage sites in *ctpA* mRNA. Primer extension was carried out as described in Materials and Methods. Each primer extension product was analyzed on a 6% sequencing gel with the DNA sequencing ladder prepared with the same primer. (A and B) Cleavage sites in *ctpA* mRNA detected with the primer pEa. (C and D) Cleavage sites in *ctpA* mRNA detected with the primer pEb. The RNA sequences complementary to the DNA sequence ladder are shown to the right of each figure, and corresponding cleavage sites are indicated by arrows.

TABLE 1. *ctpA* mRNA sequences around cleavage sites

Primer	mRNA sequence around cleavage site(s)[a]
pEa	$^{+103}$AAACGUUGGCA**AU↓UC** AUAUCAAUAUUAA^{+130} $^{+156}$CAUCACAGUU**GUU↓G** CAUAUAUUUUUAU^{+181}
pEb	$^{+221}$CAAGCAA**↓ACUU↓A** AAUAAAAUUG^{+238} $^{+250}$AAAAU**CUU↓A** AAUAGUGAUUA**UU↓A** CAAAA^{+277}
pEd	$^{+475}$CCAGCAGAACGUGCUGGCA**↓UUC** GUCC^{+502}

[a] The cleavage sites in the *ctpA* mRNA were determined by in vitro primer extension with primers pEa, pEb, and pEd (Fig. 4). The sequences around the MazF$_{sa}$ cleavage sites are indicated by bold characters, and the cleavages are indicated by arrows.

primary cleavages occur at either 5′ side of the first U or 3′ side of the second U residue in the VUUV′ sequence, with most cleavages taking place 3′ of the second U residue (Fig. 4; Table 1). However, not all of the VUUV′ sequences in the *ctpA* mRNA were cleaved by MazF$_{Sa}$.

Cleavage specificity of MazF$_{Sa}$. To further define the specificity of cleavage sites, an 18-base synthetic RNA (5′-UUGG CAAUUCAUAUCAAU-3′) with the AUUC sequence in the center was used for digestion with MazF$_{Sa}$. A clear cleavage was shown between the A and U of the sequence (Fig. 5A).

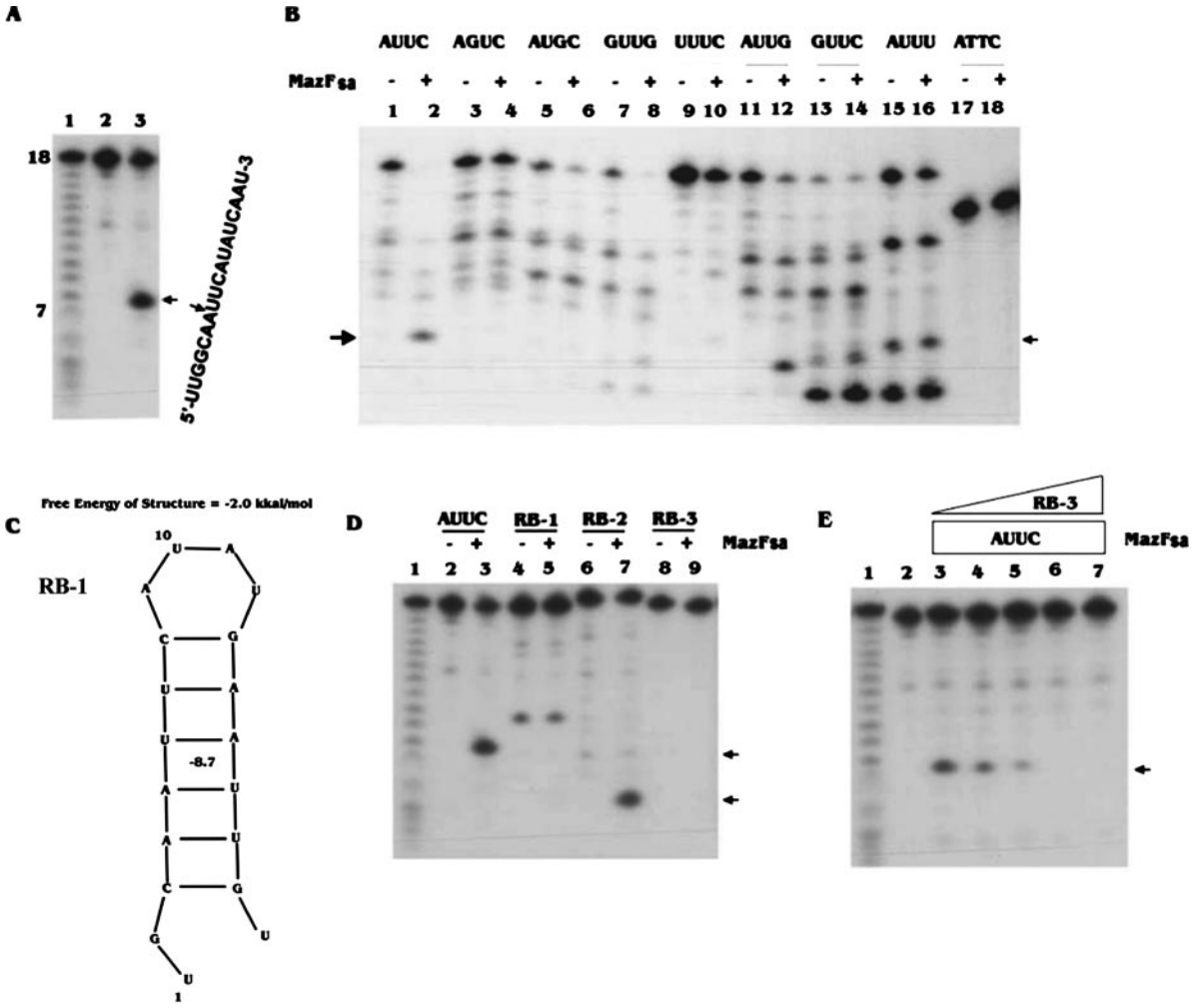

FIG. 5. Cleavage of synthetic RNA by MazF$_{Sa}$. All RNA substrates labeled at the 5′ end with [γ-^{32}P]ATP were digested with MazF$_{Sa}$ and subjected to analysis in a 20% sequencing gel run with an RNA ladder by alkaline hydrolysis as described in Materials and Methods. (A) Cleavage of a synthetic 18-base RNA, AUUC. Lane 1, RNA ladder generated by alkaline hydrolysis; lane 2, RNA substrate without the addition of MazF$_{Sa}$; lane 3, RNA substrate digested by15 pmol of MazF$_{Sa}$. The corresponding RNA sequence is shown to the right. The cleavage product and site are indicated by arrows. (B) Cleavage specificity of MazF$_{Sa}$ with synthetic 18-base RNA substrates. Seven RNA substrates with the center AUUC sequence were changed to AGUC, AUGC, GUUG, UUUC, AUUG, GUUC, and AUUU sequences and named correspondingly. The ATTC indicates the same length of DNA substrate. Lanes 1, 3, 5, 7, 9, 11, 13, 15, and 17 contained no MazF$_{Sa}$; lanes 2, 4, 6, 8, 10, 12, 14, 16, and 18 are with 15 pmol of MazF$_{Sa}$ added. The background in the absence of MazF$_{Sa}$ was attributed to impurities or incomplete synthesis of the full-length RNA substrates. Nevertheless, cleavage can be seen with MazF$_{Sa}$, as indicated by the arrows. (C) Predicted secondary structure formed by RB-1 (5′-UGCAAUUCAUAUGAAUUGU-3′) using the RNA secondary prediction website (http://www.genebee.msu.su/services/rna2_reduced.html). (D) Cleavage of highly purified synthetic RNA substrates with different secondary structures. An 18-base sense RNA, AUUC, and AUUC antisense RNA RB-3, were digested separately by MazF$_{Sa}$. The 19-base RNAs RB-1 and RB-2 (an RB-1 variant) were also digested with MazF$_{Sa}$. Lanes 2, 4, 6, and 8 are with no MazF$_{Sa}$ addition; lanes 3, 5, 7, and 9 are with 15 pmol of MazF$_{Sa}$ added. The cleavage products are indicated by arrows. (E) Effects of RNA-RNA duplex formation on cleavage by MazF$_{Sa}$. Lane 1, RNA ladder generated by alkaline hydrolysis; lane 2, labeled sense RNA alone; lane 3, labeled sense RNA digested with 15 pmol of MazF$_{Sa}$; lanes 4 to 7, the labeled 18-base sense RNA, AUUC, was annealed with AUUC antisense RNA RB-3 in ratios of 1: 0.2, 1:0.4, 1:0.8, and 1:1, respectively, as indicated and then digested with 15 pmol of MazF$_{Sa}$ at 37°C for 30 min.

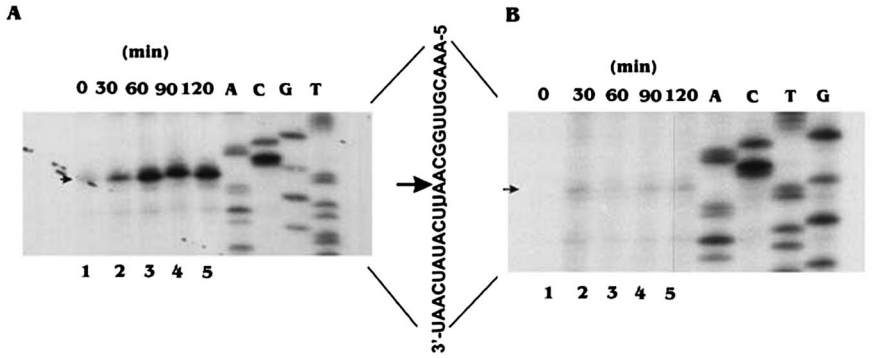

FIG. 6. In vivo cleavage of *ctpA* mRNA after induction for $MazF_{Sa}$ expression. Expression of $MazF_{Sa}$ in *E. coli* BL21(DE3)pLysS carrying plasmids pET14b-ctpA and pBAD-MazF$(His)_6$ was induced by arabinose (0.2%) (A). The expression of $MazF_{Sa}$ in *S. aureus* 178RI carrying plasmid pG164-MazF$(His)_6$/ctpA was induced by 1 mM IPTG (B). Total cellular RNAs were extracted at the indicated time points. Primer extension was then carried out as described in Materials and Methods. The DNA sequencing ladder was prepared using the same primer. The cleavage sites in the *ctpA* mRNA are indicated by arrows. The two panels represent in vivo primer extension with primer pEa from *E. coli* and *S. aureus*, respectively.

Seven additional 18-base synthetic RNA substrates were synthesized with the AUUC sequence in the center being replaced by AGUC, AUGC, AUUU, AUUG, GUUC, GUUG, or UUUC to examine consensus residues in VUUV′ (Fig. 5B). Our analyses showed that both U residues are essential for cleavage to occur; alterations in any of the two U residues in the center of the consensus sequence completely abolished the cleavage by $MazF_{Sa}$ (Fig. 5B, lanes 4 and 6). The cleavage efficiency was reduced significantly if the first and the fourth residues were changed to U (Fig. 5B, lanes 10 and 16). The fourth C residue could be changed to G without any significant loss of cleavage efficiency (Fig. 5B, lane 12). The first A could be changed to G with some degree of reduced cleavage efficiency (Fig. 5B, lanes 8 and 14). No cleavage occurred with the corresponding single-stranded DNA sequence (Fig. 5B, lane 18), indicating that $MazF_{Sa}$ specifically cleaves RNA. There was clear cleavage with the sequences AUUA and CUUA in the *ctpA* mRNA template, as shown in Fig. 4C and D. These results confirm that $MazF_{Sa}$ is an endoribonuclease that specifically cleaves the consensus RNA sequence VUUV′.

There are other VUUV′ sequences present in the *ctpA* mRNA, but cleavage did not occur with these sequences. We speculate that secondary structures of the substrate may affect the cleavage by $MazF_{Sa}$. To test this, a highly purified 19-base synthetic RNA, RB-1, which can form a hairpin structure with the AUUC sequence embedded within the stem region (Fig. 5C), was digested with $MazF_{Sa}$. Cleavage was completely blocked with this hairpin structure, whereas clear cleavage occurred with the purified RB-2, the synthetic RNA without the hairpin structure that encompassed the AUUC sequence (Fig. 5D, lanes 5 and 7). We next examined the cleavage of $MazF_{Sa}$ on the AUUC antisense RNA, RB-3. Although there was an AUUG sequence in the single-stranded AUUC antisense RNA, cleavage by $MazF_{Sa}$ did not occur (Fig. 5D, lane 9), whereas the altered sense-strand RNA with the AUUG sequence (Fig. 5B, lane 12) was efficiently cleaved by $MazF_{Sa}$. The reason for this discrepancy is unknown, but it is conceivable that the sequences adjacent to VUUV′ may play a role in promoting cleavage. The cleavage by $MazF_{Sa}$ was also blocked when the sense RNA with the AUUC sequence annealed with its antisense-strand RNA, RB-3, to form an RNA-RNA duplex in a dose-dependent manner (Fig. 5E). These results suggested that $MazF_{Sa}$ cannot cleave the VUUV′ sequences in the RNA-RNA duplex and hence is only specific for single-stranded RNA without any intramolecular base pairing involving VUUV′.

In vivo cleavage of *ctpA* RNA by $MazF_{Sa}$. To determine the $MazF_{Sa}$-specific cleavage sites in mRNA in vivo, primer extension analysis of *ctpA* mRNA was performed with total RNA extracted from both *E. coli* and *S. aureus* carrying the corresponding plasmids at various time points after induction as described in Materials and Methods. A clear in vivo cleavage site was determined in *E. coli* with primer pEa, as shown in Fig. 6A. A primer extension product appeared at 30 min after induction of $MazF_{Sa}$, with subsequent time points showing cleavage in a time-dependent manner (lanes 2 to 5). However, the effect of $MazF_{Sa}$ in *E. coli* likely occurs within seconds of initiation of the reaction, as this extension product can almost be detected at time zero (Fig. 6A, lane 1). In vivo cleavage was also detected in *S. aureus* 178RI carrying plasmid pG164-MazF$(His)_6$/ctpA with primer pEa (Fig. 6B), but the cleaved *ctpA* mRNA with the extension product was faintly detected only after 30 min of induction (Fig. 6B). We speculate this may be due to a lower copy number of the cotranscribed *ctpA* mRNA. Nevertheless, the cleavage recognition site in vivo in both *E. coli* and *S. aureus* (Fig. 6A and B) was found to be identical to the one in vitro (Fig. 4A), but the cleavage site was shifted two bases upstream. Collectively, these results indicated that $MazF_{Sa}$ recognizes the same site on *ctpA* mRNA both in vivo and in vitro, but the exact cleavage site may differ by one to two bases between those in vivo and in vitro, which could be due to trimming of the RNA ends by cellular RNases.

Environmental stress triggers increasing expression of the *$mazEF_{Sa}$* transcript. The $mazEF_{Sa}$ operon is located upstream of the *sigB* operon and is cotranscribed as a 3.6-kb transcript (Fig. 1A). This genetic arrangement suggests that $mazEF_{Sa}$ may be related to environmental stresses. We thus examined the transcription of $mazEF_{Sa}$ upon exposure to antibiotics. Increased expression of a 3.6-kb and a 0.5-kb transcript, as estimated from the migration pattern and corresponding to the

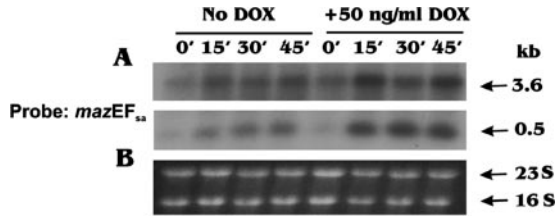

FIG. 7. DOX stress induced increasing expression of *mazEF$_{Sa}$* transcripts. The *S. aureus* Newman culture was treated with 50 ng/ml DOX at optical density at 650 nm of 1.0. Total cellular RNAs were extracted at the indicated time points. Northern blot analysis was carried out with the *mazEF$_{Sa}$* probe as described in Materials and Methods. (A) Transcripts detected with the probe. (B) 23S and 16S served as the internal loading control.

cotranscript with the *sigB* operon and the transcript of the *mazEF$_{Sa}$* operon alone (Fig. 1A), respectively, was detected with the *mazEF$_{Sa}$* probe upon exposure to doxycycline (DOX) for 45 min (Fig. 7). The increase of both transcripts was also found with exposure to sub-MIC levels of other antibiotics, e.g., erythromycin and penicillin (unpublished data). Interestingly, no reduction in CFU counts was observed with exposure to antibiotic at sub-MIC levels (data not shown). Similarly, we also found brief exposure of *S. aureus* cells to heat (48°C) activated transcription of the *mazEF$_{Sa}$* promoter (unpublished data), thus confirming the finding of Senn et al., who also demonstrated increased transcription of *mazEF$_{Sa}$* with *sigB* upon heat stress treatment (30). This is different from the *mazEF* system in *E. coli*, wherein brief exposure of antibiotic or heat disrupts *mazEF* transcription and translation, thus leading to proteolysis of the labile MazE and hence unleashing the endoribonuclease activity of MazF (1, 15, 29). This mode of action of MazF in *E. coli* has been termed programmed cell death by one group of investigators (9), but this claim has been disputed in studies presented by Tsilibaris et al. (33).

DISCUSSION

Staphylococcus aureus is a major opportunistic pathogen that is a leading cause of nosocomial infections associated with surgical wounds and indwelling medical devices. Despite antimicrobial therapy, the morbidity and mortality associated with *S. aureus* infections remain high, due in part to the organism's ability to develop resistance to antibiotics, including that to vancomycin (5, 20). In searching for antimicrobial targets within the stress-induced operon, we noticed, as did Kullik et al. (18), that the ORF (SA2058) upstream of *rsbU*, the first gene within the established *sigB* operon, shares sequence similarity with *mazF* of *E. coli*. Given that *mazE* and *mazF* in prokaryotes are often cotranscribed, we were puzzled with the functional identity of these two ORFs, since SA2059, directly upstream of SA2058, has little homology with *mazE* of *E. coli*.

In *S. aureus*, SA2059 and SA2058 have been shown to cotranscribe with the *sigB* operon, particularly under stressful conditions (30). Given that both *mazEF* and the *sigB* operons are modulated under stress and that SA2058 is homologous with *mazF* of *E. coli*, it is reasonable to speculate that SA2058 and SA2059 may represent a MazEF-like system in *S. aureus*, despite a lack of supporting experimental data. In this study, we demonstrated that MazEF$_{Sa}$ of *S. aureus* is a TA module wherein MazF$_{Sa}$ is the toxin and MazE$_{Sa}$ is the antitoxin that binds MazF$_{Sa}$ to inhibit its toxicity. Our data showed that MazF$_{Sa}$ is toxic to both *E. coli* and *S. aureus* after induction for its expression (Fig. 1). It inhibits protein synthesis in a cell-free system by cleaving mRNA substrates. MazE$_{Sa}$, on the other hand, inhibits the toxicity of MazF$_{Sa}$ by preventing cleavage of the target mRNA and hence releases the inhibition in protein synthesis by MazF$_{Sa}$ (Fig. 2 and 3). This inhibition was due to the formation of the MazE$_{Sa}$/MazF$_{Sa}$ complex (Fig. 1D), which prevents the free form of MazF$_{Sa}$ from cleaving the target RNA (Fig. 3B). However, the exact stoichiometry by which the C-terminal arm of MazE$_{Sa}$ mimics the similarly charged sugar-phosphate backbone of RNA to inhibit MazF$_{Sa}$ toxin activity by occupying the RNA binding site on the MazF$_{Sa}$ toxin as described for *E. coli* (19) will require further detailed crystal structure studies of the MazE/MazF$_{Sa}$ complex.

In *S. aureus* and some gram-positive bacteria (e.g., *B. subtilis* and *Listeria monocytogenes*), *mazEF* homologs are located immediately upstream of the *sigB* operon, which encodes σ^B, the main alternative transcription factor involved in the stress response of many gram-positive bacteria, and a series of anti-sigma factors to control the concentration of free σ^B (10, 13, 27, 30). In contrast, the *mazEF* genes in *E. coli* are located downstream of the *relA* gene. *relA* encodes a synthase for ppGpp and is upregulated in response to uncharged tRNA at the ribosomal A-site during amino acid starvation and other stressful conditions, including antibiotic exposure (1, 15, 29). It was shown that overproduction of ppGpp (by overproducing RelA′, a truncated version of ppGpp synthetase I of *E. coli*) in a strain derived from MC4100 represses expression from the *mazEF* promoter. Those authors then suggested that physiological conditions that confer increased levels of ppGpp would reduce synthesis of MazE antitoxin, hence enabling degradation of the more labile MazE antitoxin by the ClpPA protease system and unleashing the toxic effect of MazF to execute programmed cell death (PCD) (1). However, Christensen et al. (6) investigated whether the transcription pattern of *mazEF* during amino acid starvation induced by serine hydroxamate was stimulated strongly by amino acid starvation, and this stimulation depended on Lon. No TA locus-dependent cell killing was observed during this amino acid starvation. Penersen et al. (25) also showed that the toxicity of MazF in *E. coli* can be rescued by the antitoxin MazE, expressed within 6 h after MazF induction. They further proposed that MazF does not mediate cell killing but rather induces a bacteriostatic condition. Both studies have shed doubt on the notion of PCD proposed by Aizenman et al. (1). Indeed, even with the overproduction of MazF, *E. coli* cells can retain transcriptional and translational competence for 4 days despite their growth arrest (31). Although Sat et al. (29), Amitai et al. (2), and Hazan et al. (15) suggested PCD is mediated by *mazEF* from *E. coli* upon exposure to some antibiotics, controversial results were presented for the same PCD experiments by Tsilibaris et al. (33); thus, the physiological roles of the toxin proteins remain under debate.

Our results demonstrated that the expression of the *mazEF$_{Sa}$* transcripts was up-regulated (Fig. 7) when the culture was exposed to sub-MIC levels of some antibiotics, with no great loss of cell viability. Given the divergent structural ar-

rangement between *E. coli* and *S. aureus* with respect to MazEF and the stress operon, the regulation of the *S. aureus* $MazEF_{Sa}$ TA module in response to stress warrants additional investigation (unpublished data). Pedersen et al. (25) reported that RelE-induced cell stasis exhibited increased sensitivity towards environmental stresses, e.g., heat shock, oxygen radicals, and osmotic stress. The above studies have led to the suggestion that TA complexes might constitute a novel approach toward the potential development of a new class of antimicrobial compounds which activate or mimic bacterial toxins. Compounds could function through several different mechanisms, such as preventing or reducing the association between a given TA pair or manipulating the signaling pathway that leads to toxin activation (9, 12, 22).

As with *E. coli* MazF, the $MazF_{Sa}$ of *S. aureus* was also found to be a ribosome-independent endoribonuclease, but with very different sequence specificity compared with other MazF homologs. In particular, it cleaves the RNA substrate in a U-rich region with the consensus sequences VUUV′ as demonstrated both in vivo and in vitro (Fig. 4 and 5). Most commonly, the cleavage sites reside in the 5′ end of the first U residue and at the 3′ end of the second U (Fig. 4; Table 1). Importantly, the two U residues are essential for the $MazF_{Sa}$ cleavage, since replacement of either U residue abolishes the cleavage while the V and V′ residues can be A, C, and G. When V or V′ residues were changed to U, the cleavage efficiency was significantly reduced (Fig. 5). Previously, the MazF of *E. coli* was demonstrated to cleave RNA substrates specifically at the 5′ end of ACA sequences (34). Similarly, two MazF homologs from *Mycobacterium tuberculosis* were also found to cleave at UAC triplets and (U/C)U ↓ (A/U)C(U/C) in the mRNA (39). Another PemK family toxin, EndoA from *Bacillus subtilis*, which shares homology with MazF of *E. coli*, was also shown to cleave at a UAC sequence (27). These results suggest that the cleavage sites of different MazF homologs in prokaryotes can differ. In particular, $MazF_{Sa}$ is the first example of a toxin that cleaves most commonly at the 5′ or 3′ end an invariant UU residue with a consensus sequence of VUUV′. How various toxins contribute to bacterial cell physiology and metabolism in response to stress by cleaving mRNAs at specific sites is of general interest and merits further studies.

As there are other VUUV′ sequences within the *ctpA* mRNA that are not amenable to cleavage, we investigated the role of the secondary structure of RNA, including the stem-loop structure and RNA duplex, in mRNA cleavage by $MazF_{Sa}$. Our data clearly showed that the VUUV′ sequence can be cleaved as part of a loop, but not as part of the stem where the VUUV′ sequence may form a partial RNA duplex (Fig. 5C and D). To confirm this, we incubated $MazF_{Sa}$ with a perfect RNA-RNA duplex where the antisense RNA was complementary to the sense RNA strand, which is amenable to cleavage under in vitro conditions. As predicted from the stem-loop study and in concordance with the data for the MazF of *E. coli* (37), $MazF_{Sa}$ can only cleave the single-stranded RNA at the predicted VUUV′ site but not the perfect RNA-RNA duplex (Fig. 5E). Curiously, the $MazF_{Sa}$ toxin cannot cleave the complementary antisense RNA strand with the 5′-GAAU UG-3′ sequence, where the first four bases are complementary to the AUUC consensus sequence in the sense strand and the last four nucleotides constitute the putative AUUG cleavage site (see the description of the AUUC antisense RB-3 in Materials and Methods). The reason for the difference in cleavage between the sense and the AUUC antisense strand is not entirely clear, but it may be due to the secondary structure, or the adjacent sequence may contribute to recognition of the putative site. Our data also demonstrated that $MazF_{Sa}$ recognizes the same site on *ctpA* mRNA both in vivo and in vitro, but the exact cleavage site differed by one to two bases (Fig. 6). These differences may be due to changes in the buffering environment, which could affect the folding of the *ctpA* mRNA substrate. It is also quite possible that there may be another protein interacting with $MazF_{Sa}$ besides $MazE_{Sa}$, which could change the conformation of this endoribonuclease, or that the RNA ends may be trimmed by RNases in vivo.

Recently, Moritz and Hergenrother showed that the *mazEF* TA system was found to be ubiquitous among plasmids obtained from vancomycin-resistant enterococci (22). Consistent with the early discovery of TA system in plasmids (11, 24), they proposed that the MazEF system functions to stabilize the plasmid in *Enterococcus* species. Since the *vanA* gene, the critical component of vancomycin resistance in enterococci (22), resides on the same plasmid as that of the *mazEF* genes in over 90% of the strains, this raises the possibility that TA systems may also serve to maintain the vancomycin-resistant gene in *Enterococcus* species. Given that gene transfer has been shown to occur between staphylococci and enterococci, it remains to be seen if the $MazEF_{Sa}$ system plays an important role in maintenance of antibiotic resistance genes in *S. aureus*.

Although the $MazF_{Sa}$ toxin shares sequence similarity to its counterparts in *E. coli* and *B. subtilis*, the antitoxin $MazE_{Sa}$ was found to be homologous to MazE-like molecules only in *Staphylococcus epidermis*, *Staphylococcus hemolyticus* and *Staphylococcus saprophyticus*, but not to other paralogs in gram-positive species (e.g., YdcD in *B. subtilis*). Studies in another TA module called *yefM/yoeB* in *Streptococcus pneumoniae* showed that the toxicity of YoeB could be reverted by its cognate antitoxin YefM, but not by the YefM homolog from *E. coli* (23). The above findings clearly indicate that antitoxins are different between species within the same TA systems, while the toxins are more homologous.

Collectively, our findings indicate that the $MazF_{Sa}$ of *S. aureus* differs in cleavage specificity from its *E. coli* counterpart. Based on the arrangement of $mazEF_{Sa}$ together with the *sigB* operon as a single transcription unit and that the *sigB* operon is a known stress-induced transcription unit, we speculate that the toxic effect of $MazF_{Sa}$ for *S. aureus* in response to stress likely diverges from that of *E. coli*. Finally, genomic mining reveals that $MazE_{Sa}$ may be unique in staphylococcal species. Accordingly, we predict that a successful anti-$MazE_{Sa}$ strategy will be active against other staphylococcal species as well.

ACKNOWLEDGMENTS

We thank Eric Brown and Todd Black for providing *S. aureus* strain SA178RI and plasmid pG164.

This work was supported by research grants AI47441 (to A.L.C.) from NIH.

REFERENCES

1. **Aizenman, E., H. Engelberg-Kulka, and G. Glaser.** 1996. An *Escherichia coli* chromosomal "addiction module" regulated by guanosine [corrected] 3′,5′-

bispyrophosphate: a model for programmed bacterial cell death. Proc. Natl. Acad. Sci. USA **93:**6059–6063.
2. **Amitai, S., Y. Yassin, and H. Engelberg-Kulka.** 2004. MazF-mediated cell death in *Escherichia coli*: a point of no return. J. Bacteriol. **186:**8295–8300.
3. **Cheung, A. L., J. M. Koomey, C. A. Butler, S. J. Projan, and V. A. Fischetti.** 1992. Regulation of exoprotein expression in *Staphylococcus aureus* by a locus (*sar*) distinct from *agr*. Proc. Natl. Acad. Sci. USA **89:**6462–6466.
4. **Cheung, A. L., K. J. Eberhardt, and V. A. Fischetti.** 1994. A method to isolate RNA from gram-positive bacteria and mycobacteria. Anal. Biochem. **222:** 511–514.
5. **Cheung, A. L., A. S. Bayer, G. Zhang, H. Gresham, and Y. Q. Xiong.** 2004. Regulation of virulence determinants in vitro and in vivo in *Staphylococcus aureus*. FEMS Immunol. Med. Microbiol. **40:**1–9.
6. **Christensen, S. K., K. Pedersen, F. G. Hansen, and K. Gerdes.** 2003. Toxin-antitoxin loci as stress-response-elements: ChpAK/MazF and ChpBK cleave translated RNAs and are counteracted by tmRNA. J. Mol. Biol. **332:**809–819.
7. **Condon, C.** 2006. Shutdown decay of mRNA. Mol. Microbiol. **61:**573–583.
8. **D'Elia, M. A., M. P. Pereira, Y. S. Chung, W. Zhao, A. Chau, T. J. Kenney, M. C. Sulavik, T. A. Black, and E. D. Brown.** 2006. Lesions in teichoic acid biosynthesis in *Staphylococcus aureus* lead to a lethal gain of function in the otherwise dispensable pathway. J. Bacteriol. **188:**4183–4189.
9. **Engelberg-Kulka, H., R. Hazan, and S. Amitai.** 2005. mazEF: a chromosomal toxin-antitoxin module that triggers programmed cell death in bacteria. J. Cell Sci. **118:**4327–4332.
10. **Ferreira, A., M. Gray, M. Wiedmann, and K. J. Boor.** 2004. Comparative genomic analysis of the *sigB* operon in *Listeria monocytogenes* and in other gram-positive bacteria. Curr. Microbiol. **48:**39–46.
11. **Gerdes, K., P. B. Rasmussen, and S. Molin.** 1986. Unique type of plasmid maintenance function: postsegregational killing of plasmid free cells. Proc. Natl. Acad. Sci. USA **83:**3116–3120.
12. **Gerdes, K., S. K. Christensen, and A. Lobner-Olesen.** 2005. Prokaryotic toxin-antitoxin stress response loci. Nat. Rev. Microbiol. **3:**371–382.
13. **Gertz, S., S. Engelmann, R. Schmid, K. Ohlsen, J. Hacker, and M. Hecker.** 1999. Regulation of σ^B-dependent transcription of *sigB* and *asp*23 in two different *Staphylococcus aureus* strains. Mol. Gen. Genet. **261:**558–566.
14. **Guzman, L. M., D. Belin, M. J. Carson, and J. Beckwith.** 1995. Tight regulation, modulation, and high-level expression by vectors containing the arabinose P_{BAD} promoter. J. Bacteriol. **177:**4121–4130.
15. **Hazan, R., B. Sat, and H. Engelberg-Kulka.** 2004. *Escherichia coli mazEF*-mediated cell death is triggered by various stressful conditions. J. Bacteriol. **186:**3663–3669.
16. **Huang, L., P. Tsui, and M. Freundlich.** 1992. Positive and negative control of *ompB* transcription in *Escherichia coli* by cyclic AMP and the cyclic AMP receptor protein. J. Bacteriol. **174:**664–670.
17. **Kamada, K., F. Hanaoka, and S. K. Burley.** 2003. Crystal structure of the MazE/MazF complex: molecular bases of antidote-toxin recognition. Mol. Cell **11:**875–884.
18. **Kullik, I., P. Giachino, and T. Fuchs.** 1998. Deletion of the alternative sigma factor σ^B in *Staphylococcus aureus* reveals its function as a global regulator of virulence genes. J. Bacteriol. **180:**4814–4820.
19. **Li, G. Y., Y. Zhang, M. C. Chan, T. K. Mal, K. P. Hoeflich, M. Inouye, and M. Ikura.** 2006. Characterization of dual substrate binding sites in the homodimeric structure of *Escherichia coli* mRNA interferase MazF. J. Mol. Biol. **357:**139–150.
20. **Manna, A. C., and A. L. Cheung.** 2006. Expression of SarX, a negative regulator of *agr* and exoprotein synthesis, is activated by MgrA in *Staphylococcus aureus*. J. Bacteriol. **188:**4288–4299.
21. **Mittenhuber, G.** 1999. Occurrence of mazEF-like antitoxin/toxin systems in bacteria. J. Mol. Microbiol. Biotechnol. **1:**295–302.
22. **Moritz, E. M., and P. J. Hergenrother.** 2007. Toxin-antitoxin systems are ubiquitous and plasmid-encoded in vancomycin-resistant enterococci. Proc. Natl. Acad. Sci. USA **104:**311–316.
23. **Nieto, C., I. Cherny, S. K. Khoo, M. G. de Lacoba, W. T. Chan, C. C. Yeo, E. Gazit, and M. Espinosa.** 2007. The *yefM-yoeB* toxin-antitoxin systems of *E. coli* and *S. pneumoniae*: functional and structural correlation. J. Bacteriol. **189:**1266–1278.
24. **Ogura, T., and S. Hirage.** 1983. Mini-F plasmid genes that couple host cell division to plasmid proliferation. Proc. Natl. Acad. Sci. USA **80:**4784–4788.
25. **Pedersen, K., S. K. Christensen, and K. Gerdes.** 2002. Rapid induction and reversal of a bacteriostatic condition by controlled expression of toxins and antitoxins. Mol. Microbiol. **45:**501–510.
26. **Pedersen, K., A. V. Zavialov, M. Y. Pavlov, J. Elf, K. Gerdes, and M. Ehrenberg.** 2003. The bacterial toxin RelE displays codon-specific cleavage of mRNAs in the ribosomal A site. Cell **112:**131–140.
27. **Pellegrini, O., N. Mathy, A. Gogos, L. Shapiro, and C. Condon.** 2005. The *Bacillus subtilis* ydcDE operon encodes an endoribonuclease of the MazF/PemK family and its inhibitor. Mol. Microbiol. **56:**1139–1148.
28. **Sambrook, J., E. F. Fritsch, and T. Maniatis.** 1989. Molecular cloning: a laboratory manual, 2nd ed. Cold Spring Harbor Laboratory Press, Cold Spring Harbor, NY.
29. **Sat, B., R. Hazan, T. Fisher, H. Khaner, G. Glaser, and H. Engelberg-Kulka.** 2001. Programmed cell death in *Escherichia coli*: some antibiotics can trigger *mazEF* lethality. J. Bacteriol. **183:**2041–2045.
30. **Senn, M. M., P. Giachino, D. Homerova, A. Steinhuber, J. Strassner, J. Kormanec, U. Fluckiger, B. Berger-Bachi, and M. Bischoff.** 2005. Molecular analysis and organization of the σ^B operon in *Staphylococcus aureus*. J. Bacteriol. **187:**8006–8019.
31. **Suzuki, M., J. Zhang, M. Liu, N. A. Woychik, and M. Inouye.** 2005. Single protein production in living cells facilitated by an mRNA interferase. Mol. Cell **18:**253–261.
32. **Takagi, H., Y. Kakuta, T. Okada, M. Yao, I. Tanaka, and M. Kimura.** 2005. Crystal structure of archaeal toxin-antitoxin RelE-RelB complex with implications for toxin activity and antitoxin effects. Nat. Struct. Mol. Biol. **12:**327–331.
33. **Tsilibaris, V., G. Maenhaut-Michel, N. Mine, and L. Van Melderen.** 2007. What is the benefit for *Escherichia coli* of having multiple toxin-antitoxin systems in its genome? J. Bacteriol. **189:**6089–6092.
34. **Zhang, Y., J. Zhang, K. P. Hoeflich, M. Ikura, G. Qing, and M. Inouye.** 2003. MazF cleaves cellular mRNAs specifically at ACA to block protein synthesis in *Escherichia coli*. Mol. Cell **12:**913–923.
35. **Zhang, J., Y. Zhang, and M. Inouye.** 2003. Characterization of the interactions within the *mazEF* addiction module of *Escherichia coli*. J. Biol. Chem. **278:**32300–32306.
36. **Zhang, J., Y. Zhang, L. Zhu, M. Suzuki, and M. Inouye.** 2004. Interference of mRNA function by sequence-specific endoribonuclease PemK. J. Biol. Chem. **279:**20678–206784.
37. **Zhang, Y., J. Zhang, H. Hara, I. Kato, and M. Inouye.** 2005. Insights into the mRNA cleavage mechanism by MazF, an mRNA interferase. J. Biol. Chem. **280:**3143–3150.
38. **Zhang, Y., L. Zhu, J. Zhang, and M. Inouye.** 2005. Characterization of ChpBK, an mRNA interferase from *Escherichia coli*. J. Biol. Chem. **280:** 26080–26088.
39. **Zhu, L., Y. Zhang, J. S. The, J. Zhang, N. Connell, H. Rubin, and M. Inouye.** 2006. Characterization of mRNA interferases from *Mycobacterium tuberculosis*. J. Biol. Chem. **281:**18638–18643.